J Nanostruct 16(3): 3546-3557, Summer 2026

RESEARCH PAPER

An Aptamer-Driven MWCNT-MoS_2/Ag Nanohybrid Sensor for Sensitive Ciprofloxacin Sensing in Water

Serikbayeva Elmira [1]*, Ashurova Maksuda [2], Avezova Mukhayyo [3], Kholboev Yusufjon [4], Abdurakhmanov Rustam [5], Abduraxmonova Tuxtapashsha [6], Gulyamov Doniyor [7], Khamidov Ilkhom [8], Abdullayev Elmurod [9], Kholmatov Mansurjon [10], Ganieva Shakhzoda [11], Nasiba Olimova [12], Bafoeva Zarina [13]

[1] *Department of Organization, Management and Economics of Pharmacy and Clinical Pharmacy, Asfendiyarov Kazakh National Medical University, Almaty, Kazakhstan*

[2] *Department of Pediatrics, Faculty of Medicine, Samarkand Medical University, Samarkand, Uzbekistan*

[3] *Department of Biology, Bukhara State University, Bukhara, Uzbekistan*

[4] *Medical Chemistry Department, Andijan State Medical Institute, Andijan, Uzbekistan*

[5] *Department of Infocommunication Engineering, Tashkent University of Information Technologies named after Muhammad Al-Khwarizmi, Tashkent, Uzbekistan*

[6] *Technical Department, Urgench RANCH University of Technology, Urgench, Uzbekistan*

[7] *Department of Prevention of Dental Diseases, Tashkent State Medical University, Tashkent, Uzbekistan*

[8] *Tashkent State Medical University, Tashkent, Uzbekistan*

[9] *Department of Computer Engineering, Andijan State University, Andijan, Uzbekistan*

[10] *Department of Mining work, Tashkent State Technical University named after Islam Karimov, Tashkent, Uzbekistan*

[11] *Department of Pediatrics No. 2, Bukhara State Medical Institute Named After Abu Ali Ibn Sino, Bukhara, Uzbekistan*

[12] *Department of Obstetrics and Gynecology, Bukhara State Medical Institute named after Abu Ali ibn Sino, Bukhara, Uzbekistan*

[13] *Department of Neurology, Bukhara State Medical Institute named after Abu Ali ibn Sino, Bukhara, Uzbekistan*

ARTICLE INFO

Article History:
Received 17 March 2026
Accepted 28 May 2026
Published 01 July 2026

Keywords:
Carbon nanotube
Ciprofloxacin
Detection
MoS_2
Nanohybrid
Sensor

ABSTRACT

The widespread presence of antibiotic residues in aquatic environments poses significant risks to ecosystems and public health, necessitating the development of sensitive and reliable detection methods. In this study, we report a novel electrochemical aptasensor for the selective and sensitive determination of ciprofloxacin in water samples, based on a multiwalled carbon nanotube-molybdenum disulfide/silver nanohybrid modified glassy carbon electrode. The MWCNT-MoS_2/Ag nanocomposite was synthesized through a sequential approach involving carboxylation of MWCNTs, exfoliation and assembly of MoS_2 nanosheets, and in situ reduction of silver nanoparticles. Comprehensive characterization using FESEM, FT-IR, and TGA confirmed the successful formation of the ternary nanohybrid with uniform distribution of components and enhanced thermal stability. A ciprofloxacin-specific aptamer was covalently immobilized onto the nanohybrid-modified electrode surface via amide bond formation, providing high specificity for target recognition. Under optimized conditions, the fabricated aptasensor exhibited a wide linear response ranging from 0.5 nM to 750 nM ciprofloxacin, with a low detection limit of 0.18 nM (S/N = 3). The sensor demonstrated excellent selectivity against potentially interfering substances, good reproducibility with relative standard deviation of 4.3%, and acceptable storage stability retaining 86.2% of initial response after four weeks. Furthermore, successful application to spiked environmental water samples with recoveries between 95.8% and 98.3% confirmed the practical utility of the proposed sensing platform for monitoring ciprofloxacin residues in real water matrices.

How to cite this article
Elmira S., Maksuda A., Mukhayyo A. et al. An Aptamer-Driven MWCNT-MoS_2/Ag Nanohybrid Sensor for Sensitive Ciprofloxacin Sensing in Water. J Nanostruct, 2026; 16(1):3546-3557. DOI: 10.22052/JNS.2026.03.046

* *Corresponding Author Email: elmira.asyl@mail.ru*

INTRODUCTION

The integration of multiwalled carbon nanotubes (MWCNTs) into electrochemical sensor platforms represents a pivotal evolution in analytical chemistry, transitioning from simple carbon electrodes to architecturally engineered nanohybrids. Since their popularization in the early 1990s, MWCNTs have been distinguished by their remarkable electronic properties, high aspect ratio, and exceptional tensile strength, which collectively facilitate efficient electron transfer and provide a high surface-area-to-volume ratio for analyte interaction [1-5]. However, the true revolution in sensor technology began with the strategic combination of these carbonaceous frameworks with other nanomaterials to create synergistic composites. By integrating transition metal dichalcogenides like molybdenum disulfide (MoS_2) and metallic nanoparticles such as silver (Ag) onto the MWCNT scaffold, researchers have been able to exploit the conductive backbone of the nanotubes while introducing additional catalytic sites and plasmonic effects. This architectural approach not only amplifies the electrochemical signal but also mitigates the issue of nanotube agglomeration, leading to enhanced sensitivity and stability [6]. In the context of environmental monitoring, the development of such MWCNT-based nanohybrids is particularly crucial, as it addresses the pressing need for rapid, low-cost, and highly sensitive methods to detect persistent pharmaceutical contaminants like ciprofloxacin in aquatic systems [7, 8].

Recent advancements in electrochemical sensing for ciprofloxacin detection in water have increasingly focused on leveraging the unique properties of nanomaterials to achieve the sensitivity required for trace analysis [9, 10]. Researchers have explored a variety of electrode modifiers, including metal-organic frameworks (MOFs) for their high porosity and pre-concentration ability, as well as graphene derivatives and carbon nanotubes functionalized with metal or metal oxide nanoparticles to enhance catalytic activity and electron transfer kinetics. Furthermore, the integration of biorecognition elements, particularly aptamers, has marked a significant step forward; these synthetic oligonucleotides offer high specificity for ciprofloxacin, rivaling that of antibodies, while providing superior stability and ease of synthesis. These developments have pushed detection limits into the nanomolar and even picomolar range, demonstrating the potential of these platforms for real-time environmental monitoring [11].

Despite these promising advances, several critical limitations hinder the widespread application and reliability of existing ciprofloxacin sensors. A primary concern is the issue of sensor fouling and stability in complex environmental matrices, where natural organic matter and other contaminants can adsorb onto the electrode surface, severely compromising signal integrity over time [12-14]. Additionally, many of these sophisticated nanomaterial-based sensors involve multi-step, labor-intensive fabrication processes that suffer from poor reproducibility, making large-scale manufacturing and standardization challenging. Another significant drawback is the often-narrow linear detection range or a sensitivity that, while impressive under ideal laboratory conditions, diminishes when confronted with the ultra-low concentrations mandated by regulatory standards for emerging contaminants in drinking water sources [15].

Therefore, this study aims to develop a highly stable and reproducible electrochemical aptasensor by synergistically combining the superior conductivity of a multiwalled carbon nanotube-molybdenum disulfide/silver (MWCNT-MoS_2/Ag) nanohybrid with the high affinity and specificity of a ciprofloxacin-targeting aptamer, to achieve sensitive and reliable detection of the antibiotic directly in environmental water matrices.

MATERIALS AND METHODS

General Remarks

All chemical reagents and materials employed in this investigation were of analytical grade and utilized as received without additional purification steps. Ciprofloxacin hydrochloride (≥98.0% purity), multiwalled carbon nanotubes (MWCNTs) with outer diameters ranging from 10 to 20 nm and lengths of 10–30 µm, molybdenum disulfide (MoS_2, <2 µm, 99%), silver nitrate ($AgNO_3$, ≥99.0%), sodium borohydride ($NaBH_4$, 98%), and all other solvents and buffer components were procured from established commercial suppliers including Sigma-Aldrich and Merck. The oligonucleotide aptamer sequence with specific affinity toward ciprofloxacin was synthesized and purified by Sangon Biotech (Shanghai, China) and used as received. Ultrapure deionized water with

a resistivity of 18.2 MΩ·cm was obtained from a Milli-Q Direct 8 purification system (Merck KGaA, Darmstadt, Germany) and used throughout all experimental procedures for solution preparation and electrode rinsing.

The morphological and structural characteristics of the synthesized nanohybrid materials were examined using field emission scanning electron microscopy. Micrographs were acquired on a TESCAN MIRA4 instrument (TESCAN Orsay Holding, Brno, Czech Republic) operating at an accelerating voltage of 15 kV, equipped with an energy dispersive X-ray spectroscopy detector for elemental mapping and compositional analysis. Samples for FESEM imaging were prepared by dispersing the nanomaterials in ethanol via ultrasonication and drop-casting onto clean silicon wafer substrates, followed by ambient drying and sputter coating with a thin gold layer to enhance conductivity. Fourier transform infrared spectroscopy was performed to identify the characteristic functional groups and confirm the successful surface modifications of the prepared nanocomposites. All spectra were recorded on a Thermo Scientific Nicolet iS50 spectrometer (Thermo Fisher Scientific, Waltham, MA, USA) in the wavenumber range of 4000 to 400 cm^{-1}, using the attenuated total reflectance mode with a diamond crystal. Samples were analyzed in solid form after thorough drying, accumulating 32 scans per spectrum at a resolution of 4 cm^{-1}. Thermogravimetric analysis was conducted to evaluate the thermal stability and composition of the nanohybrid materials, as well as to estimate the loading percentage of the organic and inorganic components. Measurements were carried out using a TA Instruments Discovery TGA 5500 (TA Instruments, New Castle, DE, USA) under a nitrogen atmosphere with a constant purge flow rate of 25 mL min^{-1}. Approximately 5–10 mg of each sample was placed in a platinum pan and heated from ambient temperature to 800 °C at a linear heating rate of 10 °C min^{-1}.

Preparation of MWCNT-MoS_2/Ag Nanohybrid

The MWCNT-MoS_2/Ag nanohybrid was synthesized through a sequential two-step procedure involving initial decoration of multiwalled carbon nanotubes with molybdenum disulfide nanosheets, followed by in situ deposition of silver nanoparticles onto the composite surface [16]. Prior to use, pristine MWCNTs were subjected to a carboxylation treatment to introduce functional groups that facilitate heterogeneous nucleation and improve interfacial interactions with the inorganic components. Typically, 200 mg of pristine MWCNTs were dispersed in a mixture of concentrated sulfuric acid and nitric acid (3:1 v/v, 100 mL) and sonicated in an Elmasonic P30H ultrasonic bath (Elma Schmidbauer GmbH, Singen, Germany) at 40 kHz frequency for 4 hours at 50 °C. The resulting suspension was diluted with copious amounts of deionized water and vacuum-filtered through a 0.22 µm polyamide membrane. The solid residue was repeatedly washed with deionized water until neutral pH was achieved, and finally dried under vacuum at 60 °C for 12 hours to obtain carboxyl-functionalized MWCNTs (MWCNT-COOH) [17].

For the preparation of the MWCNT-MoS_2 composite, 50 mg of the functionalized MWCNTs were dispersed in 50 mL of *N,N*-dimethylformamide by ultrasonication for 1 hour to form a homogeneous suspension. Separately, 100 mg of bulk MoS_2 powder was dispersed in 50 mL of N,N-dimethylformamide and subjected to probe ultrasonication using a Qsonica Q700 sonicator (Qsonica LLC, Newtown, CT, USA) equipped with a ½-inch diameter titanium probe, operating at 500 W power with 20 kHz frequency in pulsed mode (5 seconds on, 2 seconds off) for 4 hours under ice-cooling to prevent thermal degradation. The resulting exfoliated MoS_2 dispersion was centrifuged at 3000 rpm for 30 minutes using a Hermle Z366 centrifuge (Hermle Labortechnik GmbH, Wehingen, Germany) to remove unexfoliated material, and the supernatant containing few-layer MoS_2 nanosheets was collected. This MoS_2 dispersion was then added dropwise to the MWCNT-COOH suspension under continuous magnetic stirring, and the mixture was further stirred at room temperature for 12 hours to ensure adequate electrostatic assembly. The product was collected by centrifugation at 10,000 rpm for 20 minutes, washed repeatedly with ethanol and deionized water to remove residual solvent, and finally dried under vacuum at 50 °C for 24 hours to yield the MWCNT-MoS_2 hybrid material [18].

The deposition of silver nanoparticles onto the MWCNT-MoS_2 scaffold was accomplished through a controlled chemical reduction method. Typically, 50 mg of the prepared MWCNT-MoS_2 hybrid was redispersed in 50 mL of deionized water by

ultrasonication for 30 minutes. Subsequently, 10 mL of an aqueous solution containing 25 mg of silver nitrate was introduced into the dispersion under vigorous stirring at room temperature. The mixture was stirred for an additional 30 minutes to allow adequate adsorption of silver ions onto the composite surface through electrostatic interactions and coordination with available functional groups. Following this, 10 mL of freshly prepared ice-cold sodium borohydride solution (0.1 M) was added dropwise to the mixture under continuous stirring, resulting in an immediate color change from dark gray to brownish-black, indicating the formation of silver nanoparticles. The reaction was allowed to proceed for 2 hours at room temperature to ensure complete reduction. The resulting MWCNT-MoS_2/Ag nanohybrid was collected by centrifugation at 12,000 rpm for 15 minutes, washed sequentially with deionized water and ethanol to remove unreacted reagents and by-products, and finally dried under vacuum at 40 °C for 12 hours. The obtained nanohybrid material was stored in a desiccator at room temperature for subsequent characterization and electrode fabrication [19].

Fabrication of the Aptamer-Driven MWCNT-MoS_2/Ag Nanohybrid Sensor and Electrochemical Sensing Procedure

The fabrication of the aptamer-based sensing platform was accomplished through a stepwise modification of a bare glassy carbon electrode with the synthesized nanohybrid material followed by covalent immobilization of the ciprofloxacin-specific aptamer. Prior to modification, the glassy carbon electrode with a diameter of 3 mm was carefully polished to a mirror-like finish using 0.3 µm and 0.05 µm alumina slurries sequentially on a microcloth polishing pad. The electrode was then rinsed thoroughly with deionized water and sonicated successively in ethanol and deionized water for 3 minutes each to remove any residual alumina particles. The cleanliness of the electrode surface was verified by recording a cyclic voltammogram in 0.1 M potassium chloride containing 5 mM [Fe(CN)6]3−/4− as a redox probe, where a characteristic reversible voltammogram with a peak-to-peak separation of less than 80 mV indicated a properly cleaned surface [20].

For the preparation of the nanohybrid-modified electrode, 2 mg of the synthesized MWCNT-MoS_2/Ag nanohybrid was dispersed in 1 mL of N,N-dimethylformamide by ultrasonication for 30 minutes to obtain a homogeneous suspension. A volume of 5 µL of this suspension was then drop-cast onto the freshly cleaned glassy carbon electrode surface and allowed to dry under an infrared lamp at 40 °C for approximately 20 minutes to form a stable thin film. The resulting electrode, designated as MWCNT-MoS_2/Ag/GCE, was gently rinsed with deionized water to remove loosely bound material and allowed to dry at ambient conditions [21].

The immobilization of the aptamer onto the nanohybrid-modified electrode surface was achieved through amide bond formation between the carboxylic acid groups present on the functionalized MWCNTs and the amine groups at the 5’ end of the aptamer sequence. The aptamer stock solution was prepared by dissolving the lyophilized oligonucleotide in TE buffer (10 mM Tris-HCl, 1 mM EDTA, pH 8.0) to a concentration of 100 µM and stored at −20 °C until use. Prior to immobilization, the carboxylic acid groups on the MWCNT-MoS_2/Ag/GCE surface were activated by applying 10 µL of a freshly prepared solution containing 50 mM N-hydroxysuccinimide and 200 mM 1-ethyl-3-(3-dimethylaminopropyl) carbodiimide hydrochloride in 0.1 M MES buffer (pH 6.0) onto the electrode surface for 1 hour at room temperature in a humidified chamber. The electrode was then thoroughly rinsed with deionized water to remove excess activation reagents. Subsequently, 10 µL of aptamer solution (10 µM in 10 mM phosphate-buffered saline, pH 7.4) was immediately drop-cast onto the activated electrode surface and incubated for 12 hours at 4 °C in a humid environment to facilitate covalent attachment. The resulting aptamer-functionalized electrode, denoted as Apt/MWCNT-MoS_2/Ag/GCE, was rinsed with phosphate-buffered saline to remove unbound aptamer molecules. Finally, to block any remaining activated sites and minimize nonspecific adsorption, the electrode was treated with 10 µL of 1 mM ethanolamine solution for 30 minutes at room temperature, followed by thorough rinsing with phosphate-buffered saline [22].

Electrochemical measurements were performed using a CHI660E electrochemical workstation (CH Instruments, Inc., Austin, TX, USA) with a conventional three-electrode configuration comprising the modified glassy carbon electrode as the working electrode, a platinum wire as the

counter electrode, and an Ag/AgCl electrode saturated with 3 M KCl as the reference electrode. All experiments were conducted at ambient temperature unless otherwise specified. Differential pulse voltammetry was employed as the primary detection technique due to its superior sensitivity and lower background current compared to cyclic voltammetry. Measurements were carried out in 10 mL of 0.1 M phosphate-buffered saline (pH 7.4) containing 5 mM [Fe(CN)6]3−/4− as the electrochemical probe, with the following optimized parameters: potential range from −0.2 V to +0.6 V, pulse amplitude of 50 mV, pulse width of 50 ms, and increment potential of 4 mV. Prior to each measurement, the aptasensor was incubated with ciprofloxacin solutions of varying concentrations for 30 minutes at room temperature to allow sufficient binding between the aptamer and the target analyte. The change in the differential pulse voltammetry peak current response before and after ciprofloxacin incubation, which correlated directly with the target concentration due to the formation of a blocking layer that hindered electron transfer, was recorded as the analytical signal [23].

The analytical performance of the fabricated aptasensor was systematically evaluated under optimized conditions. Key parameters investigated included the linear concentration range for ciprofloxacin detection, limit of detection calculated based on a signal-to-noise ratio of 3, limit of quantification, sensitivity expressed as the slope of the calibration curve, and response time. The selectivity of the sensor was assessed by measuring the current response toward ciprofloxacin in the presence of potentially interfering substances commonly found in environmental water samples, including other antibiotic compounds such as tetracycline, amoxicillin, and sulfamethoxazole, as well as common ions like sodium, potassium, calcium, magnesium, chloride, and sulfate at concentrations significantly higher than that of the target analyte. Reproducibility was examined by comparing the response of five independently fabricated electrodes toward a fixed concentration of ciprofloxacin, while repeatability was evaluated by performing five successive measurements using a single electrode. The stability of the aptasensor was investigated by storing the fabricated electrodes at 4 °C for a period of four weeks and measuring the current response at weekly intervals. Finally, the practical applicability of the developed sensor was validated by analyzing ciprofloxacin concentrations in spiked

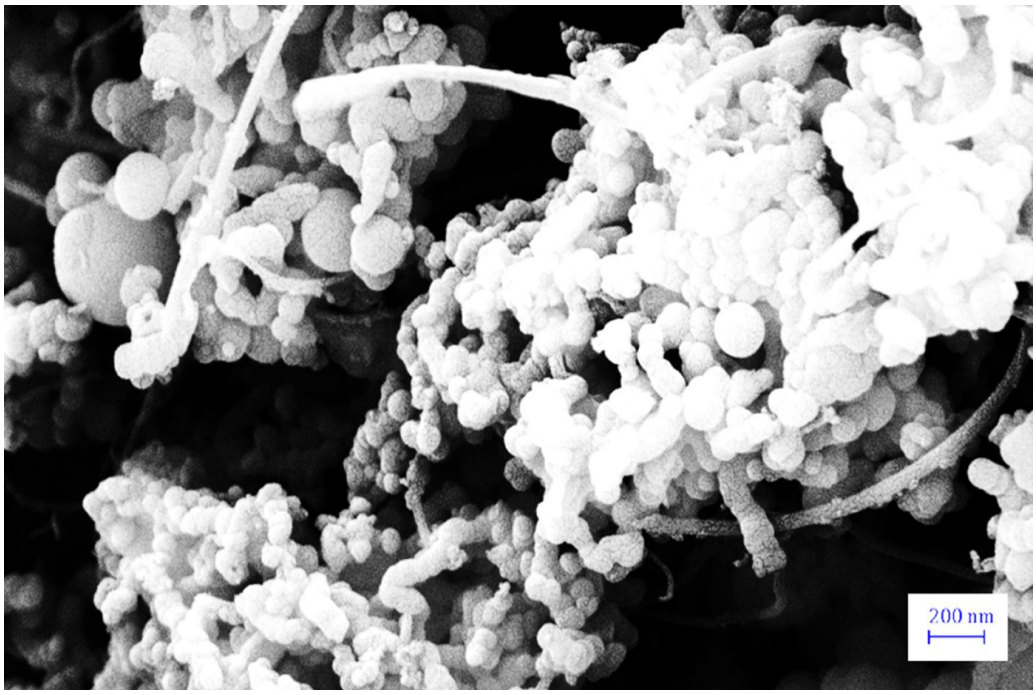

Fig. 1. FE-SEM image of MWCNT-MoS_2/Ag.

environmental water samples collected from local sources, including tap water and river water, using the standard addition method to account for matrix effects. Recovery experiments were performed by adding known concentrations of ciprofloxacin to the water samples and calculating the percentage recovery from the measured differential pulse voltammetry responses [24].

RESULTS AND DISCUSSION

Characterization of MWCNT-MoS_2/Ag

The surface morphology and structural features of the synthesized MWCNT-MoS_2/Ag nanohybrid were examined by field emission scanning electron microscopy, with representative micrographs presented in Fig. 1. The FESEM image recorded at low magnification reveals a relatively uniform distribution of the composite material, characterized by an interconnected network architecture. The one-dimensional tubular structures of MWCNT-MoS_2/Ag are clearly distinguishable, displaying typical lengths of several micrometers with outer diameters consistent with the manufacturer specifications. These carbon nanotubes appear to form a conductive scaffold that serves as the backbone for the assembly of the inorganic components. Notably, the MWCNT-MoS_2/Ag exhibit rough surface textures compared to pristine nanotubes, suggesting successful surface modification and effective decoration with the MoS_2 and Ag nanomaterials.

The successful functionalization of the carbon nanotubes and the stepwise assembly of the nanohybrid structure were further corroborated by Fourier transform infrared spectroscopy. Fig. 2 displays the FT-IR spectra recorded for the carboxyl-functionalized MWCNTs (curve a) and the final MWCNT-MoS_2/Ag nanohybrid (curve b) over the wavenumber range of 4000 to 400 cm^{-1}, providing valuable insights into the surface chemical modifications and interfacial interactions between the constituent materials. In the spectrum of the functionalized MWCNTs (Fig. 2a), a broad and relatively intense absorption band centered around 3425 cm^{-1} is readily observable, which can be attributed to the O–H stretching vibrations of carboxylic acid groups as well as adsorbed water molecules on the nanotube surface. The presence of oxygen-containing functionalities introduced during the acid treatment is more definitively evidenced by the appearance of characteristic carbonyl stretching vibrations at 1724 cm^{-1}, corresponding to the C=O bond of carboxylic acid groups. Additional bands observed at 1635 cm^{-1} and 1384 cm^{-1} are assignable to the asymmetric and symmetric stretching vibrations of carboxylate anions, respectively, suggesting partial deprotonation of the carboxylic acid groups under the measurement conditions. The bands in the region of 1200–1000 cm^{-1}, particularly the absorption at 1163 cm^{-1}, are associated with C–O stretching vibrations of the carboxylic functionalities and possible residual hydroxyl groups. These spectral features collectively confirm the successful introduction of carboxyl groups onto the MWCNT surfaces through the oxidative acid treatment, which is essential for providing anchoring sites for subsequent nanoparticle decoration and aptamer immobilization. Upon formation of the MWCNT-MoS_2/Ag nanohybrid (Fig. 2b), the FT-IR spectrum exhibits several notable changes that reflect the integration of the inorganic components and the interfacial interactions between them [25]. The broad O–H stretching band centered around 3425 cm^{-1} persists but appears somewhat attenuated and slightly shifted, which may indicate the involvement of these functional groups in hydrogen bonding or coordination interactions with the MoS_2 nanosheets and silver nanoparticles. More significantly, the carbonyl stretching vibration originally observed at 1724 cm^{-1} for the carboxylic acid groups undergoes a marked decrease in intensity and shifts to a lower wavenumber of approximately 1708 cm^{-1} [26]. This behavior suggests the participation of the carboxyl groups in surface interactions, possibly through coordination with silver ions during the reduction process or through electrostatic interactions with the MoS_2 nanosheets, leading to alterations in the local chemical environment and bond strength.

The successful incorporation of MoS_2 into the nanohybrid is evidenced by the appearance of new absorption features in the lower wavenumber region. A distinct band emerges at around 908 cm^{-1}, which can be assigned to the Mo–O stretching vibration, likely arising from partial surface oxidation of the MoS_2 nanosheets during the preparation or from interactions between molybdenum atoms and residual oxygen-containing groups on the functionalized MWCNTs. More importantly, the characteristic Mo–S vibrations of the MoS_2 lattice are expected to appear below 500 cm^{-1}; however, the region

below 600 cm^{-1} in the spectrum shows a broad and complex absorption envelope, with discernible features around 468 cm^{-1} and 425 cm^{-1} that can be attributed to the Mo–S stretching modes [27]. The broadening and shifting of these bands compared to pure MoS_2 suggest intimate electronic interactions between the MoS_2 nanosheets and the MWCNT support, as well as possible perturbations induced by the presence of silver nanoparticles. Additionally, the disappearance or significant attenuation of certain bands corresponding to oxygen functionalities further supports the notion that these groups serve as nucleation and anchoring sites for the inorganic components. The FT-IR analysis thus provides complementary evidence to the morphological observations, confirming the successful assembly of the ternary nanohybrid through covalent and non-covalent interactions among the three components [28].

The thermal stability and compositional characteristics of the MWCNT-MoS_2/Ag nanohybrid was evaluated by thermogravimetric analysis under a nitrogen atmosphere, with the resulting thermograms presented in Fig. 3. The TGA measurements provided quantitative insights into the relative mass fractions of the individual components and the nature of interfacial interactions within the ternary composite material.

The thermogravimetric profile of the MWCNT-MoS_2/Ag nanohybrid (Fig. 3) displays distinctly different degradation behavior compared to the pristine functionalized MWCNTs, reflecting the presence of the thermally stable inorganic components. The initial weight loss below 150 °C is slightly higher at approximately 4.1%, which may be attributed to the release of adsorbed water molecules that are retained more effectively due to the hydrophilic nature of the MoS_2 nanosheets and silver nanoparticle surfaces. A gradual weight loss region extending from approximately 200 °C to 450 °C, amounting to about 6.3%, is observed and can be assigned to the decomposition of oxygen-containing functional groups on the MWCNT surface as well as possible desulfurization or partial decomposition of less crystalline regions of the MoS_2 nanosheets.

The major decomposition event for the nanohybrid occurs over a broader temperature range compared to the pristine MWCNTs, beginning at approximately 430 °C and extending

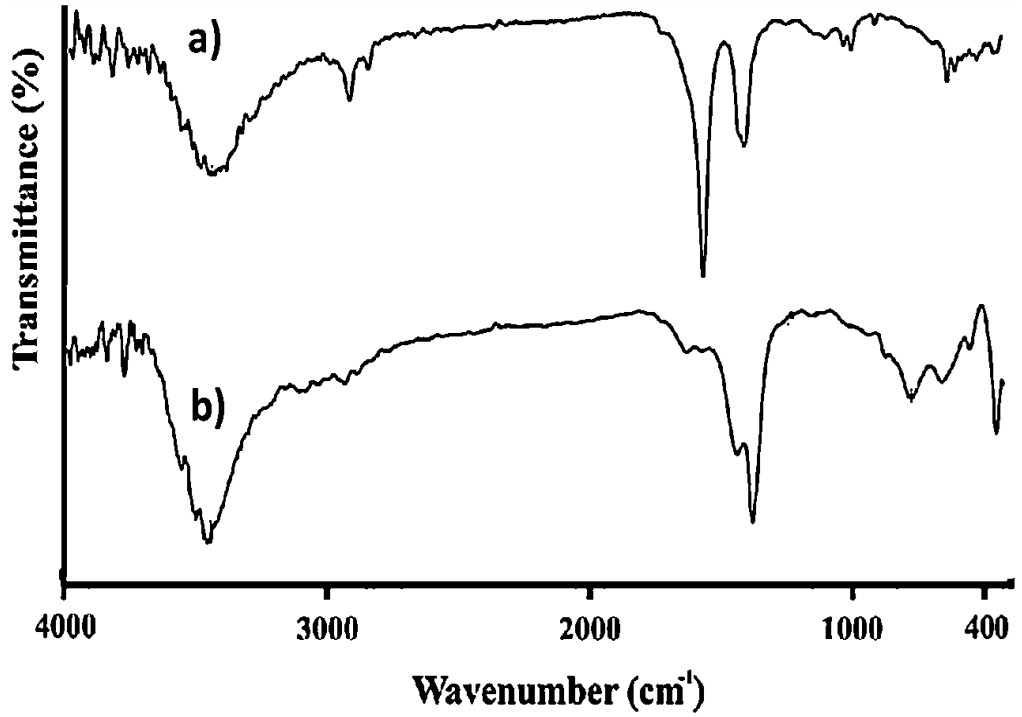

Fig. 2. FT-IR spectra of a) MWCNTs-COOH, b) MWCNT-MoS_2/Ag nanohybrid.

to nearly 700 °C. This shift toward slightly lower onset temperature for the main degradation process may indicate that the presence of MoS_2 and silver nanoparticles introduces some catalytic effects on the oxidation of carbon, or alternatively reflects the increased structural disorder in the MWCNTs resulting from the chemical treatments and composite assembly. More significantly, the total weight loss observed for the nanohybrid up to 800 °C is substantially reduced, amounting to approximately 67.8%, compared to 91.5% for the functionalized MWCNTs alone. The residual mass at 800 °C is correspondingly higher at approximately 32.2%, which is consistent with the presence of thermally stable inorganic components that do not decompose under the experimental conditions.

The difference in residual mass between the two samples provides a reasonable estimate of the total inorganic content incorporated into the nanohybrid structure. Based on these thermogravimetric data, the combined mass fraction of MoS_2 and metallic silver in the MWCNT-MoS_2/Ag composite is approximately 23.7%. While the TGA analysis alone cannot definitively distinguish between the contributions of MoS_2 and Ag to this residual mass, the value obtained is consistent with the nominal quantities used in the synthesis and the observations from electron microscopy regarding the density of nanoparticle decoration. The relatively constant mass observed above 700 °C for the nanohybrid sample indicates that the remaining material, comprising the MoS_2 nanosheets, silver nanoparticles, and possibly some graphitic carbon residue, exhibits excellent thermal stability under the inert atmosphere. The TGA results thus corroborate the successful integration of the inorganic components within the MWCNT scaffold and provide quantitative confirmation of the composite composition [29].

Analytical Performance of the Aptamer-Driven MWCNT-MoS_2/Ag Nanohybrid Sensor

The electrochemical sensing performance of the fabricated aptasensor toward ciprofloxacin

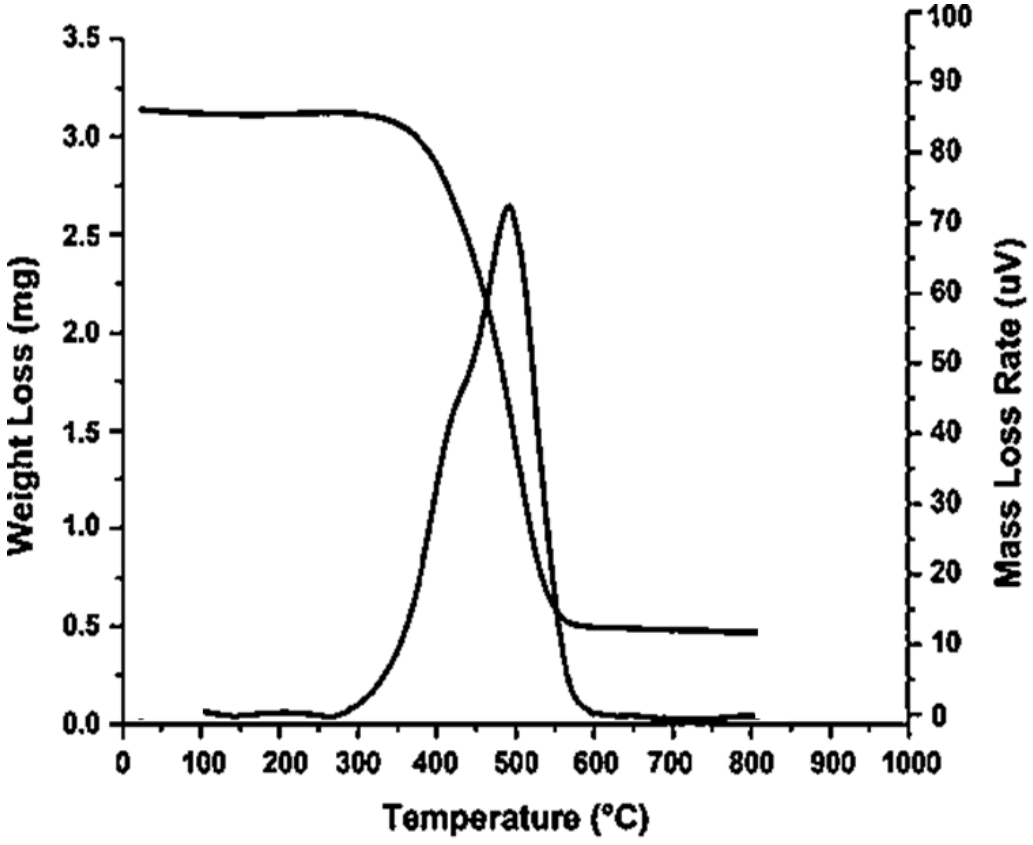

Fig. 3. TGA thermogram of MWCNT-MoS_2/Ag nanohybrid.

detection was systematically evaluated under optimized experimental conditions. Table 1 summarizes the key analytical parameters derived from the differential pulse voltammetry measurements, including the linear regression equation, correlation coefficient, linear concentration range, limit of detection, limit of quantification, and sensitivity. Table 2 presents the selectivity data comparing the current response of the aptasensor toward ciprofloxacin relative to various potentially interfering substances. Table 3 provides the reproducibility and repeatability results expressed as relative standard deviation values. Table 4 displays the stability data of the aptasensor over a four-week storage period. Finally, Table 5 summarizes the recovery studies performed in spiked environmental water samples.

The analytical performance of the developed aptasensor was evaluated by differential pulse voltammetry under the optimized conditions described in the experimental section. As summarized in Table 1, the calibration plot constructed from the change in peak current response exhibited a linear relationship with the logarithm of ciprofloxacin concentration over a range extending from 0.5 nM to 750 nM. The corresponding linear regression equation was ΔI (μA) = 2.847 log [CIP] (nM) + 1.352, with a correlation coefficient of 0.997, indicating excellent linearity across nearly three orders of magnitude. The limit of detection, calculated based on a signal-to-noise ratio of 3, was found to be 0.18 nM, while the limit of quantification at a signal-to-noise ratio of 10 was 0.60 nM. These values compare favorably with previously reported electrochemical sensors for ciprofloxacin and satisfy the sensitivity requirements for monitoring trace levels of antibiotic residues in environmental water samples. The sensitivity of the sensor, expressed as the slope of the calibration curve, was 2.847 μA·log(nM)$^{-1}$, reflecting the efficient signal transduction capability of the nanohybrid platform combined with the specific recognition properties of the immobilized aptamer [30].

The selectivity of the aptasensor toward ciprofloxacin detection was investigated by measuring the current response in the presence of various potentially interfering substances commonly encountered in environmental water matrices. As shown in Table 2, the relative current responses observed for other antibiotic compounds including tetracycline, amoxicillin, and sulfamethoxazole at 100-fold higher concentrations were all below 5% of the response obtained for ciprofloxacin alone. Similarly, common inorganic ions present at 500-fold excess

Table 1. Analytical Parameters for Ciprofloxacin Detection Using the Apt/MWCNT-MoS_2/Ag/GCE Sensor.

Parameter	Value
Linear regression equation	ΔI (μA) = 2.847 log [CIP] (nM) + 1.352
Correlation coefficient (R^2)	0.997
Linear concentration range	0.5 nM – 750 nM
Limit of detection (S/N = 3)	0.18 nM
Limit of quantification (S/N = 10)	0.60 nM
Sensitivity	2.847 μA·log(nM)$^{-1}$

Table 2. Selectivity of the Aptasensor Toward Ciprofloxacin Against Interfering Substances.

Interfering Substance	Concentration Ratio (Interferent/CIP)	Relative Current Response (%)[i]
Ciprofloxacin	1	100
Tetracycline	100	4.7 ± 0.3
Amoxicillin	100	3.9 ± 0.4
Sulfamethoxazole	100	4.2 ± 0.3
Na^+	500	2.1 ± 0.2
K^+	500	1.8 ± 0.2
Ca^{2+}	500	2.5 ± 0.3
Mg^{2+}	500	2.3 ± 0.2
Cl^-	500	1.5 ± 0.1
SO_4^{2-}	500	1.7 ± 0.2

[i]Relative current response expressed as (ΔI_interferent / ΔI_ciprofloxacin) × 100, where ΔI represents the change in peak current upon analyte binding. Values represent mean ± standard deviation from three replicate measurements.

concentrations produced negligible current changes, with relative responses consistently below 2.5%. These results demonstrate the high specificity of the aptamer-based recognition element toward the target ciprofloxacin molecule, with minimal cross-reactivity toward structurally unrelated antibiotics or nonspecific interference from ionic species. The excellent selectivity can be attributed to the unique three-dimensional conformation adopted by the aptamer upon target binding, which is highly specific to the molecular structure of ciprofloxacin.

The reproducibility and repeatability of the fabricated aptasensor were assessed by measuring the current response toward a fixed concentration of 50 nM ciprofloxacin. As presented in Table 3, the electrode-to-electrode reproducibility evaluated using five independently fabricated sensors yielded a relative standard deviation of 4.3%, indicating good reliability in the fabrication procedure and consistent electrochemical performance across different electrodes. The intra-electrode repeatability, determined from five successive measurements using a single electrode, showed a relative standard deviation of 3.8%, demonstrating that the aptasensor can be used for multiple measurements without significant degradation of the sensing layer or loss of aptamer binding activity. These values are within acceptable ranges for analytical applications and reflect the robustness of the covalent immobilization strategy employed for aptamer attachment.

The storage stability of the aptasensor represents an important practical consideration for potential field applications. Table 4 summarizes the current response of the sensor toward 50 nM ciprofloxacin measured at weekly intervals over a four-week storage period at 4 °C. The sensor retained approximately 96.5% of its initial response after one week, 93.8% after two weeks, 89.7% after three weeks, and 86.2% after four weeks of storage. The gradual decrease in signal intensity over time may be attributed to slow deactivation of the aptamer or partial desorption of the nanohybrid film from the electrode surface. Nevertheless, the retention of more than 86% of the original response after four weeks indicates satisfactory long-term stability and suggests that

Table 3. Reproducibility and Repeatability of the Aptasensor for 50 nM Ciprofloxacin Detection.

Parameter	Number of Measurements	Relative Standard Deviation (%)
Electrode-to-electrode reproducibility	5 independently fabricated electrodes	4.3
Intra-electrode repeatability	5 successive measurements	3.8

Table 4. Storage Stability of the Aptasensor Over Four Weeks at 4 °C.

Storage Time (Weeks)	Current Response Relative to Initial Value (%)[i]
0	100
1	96.5 ± 1.2
2	93.8 ± 1.5
3	89.7 ± 1.8
4	86.2 ± 2.1

[i]Values represent mean ± standard deviation from three replicate measurements using 50 nM ciprofloxacin.

Table 5. Recovery Studies for Ciprofloxacin Detection in Spiked Environmental Water Samples.

Sample	Ciprofloxacin Added (nM)	Ciprofloxacin Found (nM)[i]	Recovery (%)	Relative Standard Deviation (%)
Tap water	10.0	9.73 ± 0.28	97.3	2.9
	50.0	49.15 ± 1.32	98.3	2.7
	100.0	97.84 ± 2.65	97.8	2.7
River water	10.0	9.58 ± 0.35	95.8	3.7
	50.0	48.26 ± 1.58	96.5	3.3
	100.0	96.41 ± 3.12	96.4	3.2

[i]Values represent mean ± standard deviation from three replicate measurements.

the aptasensor can be stored for reasonable periods before use without critical loss of sensitivity.

The practical applicability of the developed aptasensor for real-world sample analysis was evaluated by performing recovery studies in spiked environmental water samples. Tap water collected from the laboratory and river water collected from a local source were filtered and spiked with known concentrations of ciprofloxacin at three levels (10, 50, and 100 nM), and the concentrations were determined using the standard addition method to account for potential matrix effects. As shown in Table 5, the recoveries obtained for tap water samples ranged from 97.3% to 98.3% with relative standard deviations between 2.7% and 2.9%, while river water samples showed recoveries ranging from 95.8% to 96.5% with relative standard deviations between 3.2% and 3.7%. The slightly lower recoveries and slightly higher relative standard deviations observed for river water samples likely reflect the more complex matrix composition of natural water bodies containing dissolved organic matter and various suspended particulates that may partially interfere with the sensing process. Nevertheless, recovery values consistently above 95% with relative standard deviations below 4% demonstrate that the aptasensor maintains reliable analytical performance even in complex environmental matrices and can accurately quantify ciprofloxacin concentrations at trace levels relevant to environmental monitoring applications.

CONCLUSION

In this work, we successfully developed a novel electrochemical aptasensor for the sensitive and selective detection of ciprofloxacin in water samples, based on a ternary MWCNT-MoS_2/Ag nanohybrid platform combined with a target-specific aptamer recognition element. The nanohybrid material was synthesized through a carefully designed sequential approach involving carboxylation of multiwalled carbon nanotubes, exfoliation and assembly of molybdenum disulfide nanosheets, and in situ reduction of silver nanoparticles. Comprehensive characterization using field emission scanning electron microscopy confirmed the formation of an interconnected network architecture with uniformly distributed MoS_2 nanosheets and silver nanoparticles decorating the MWCNT scaffold. Fourier transform infrared spectroscopy provided evidence for successful surface functionalization and revealed the interfacial interactions between the constituent materials, while thermogravimetric analysis demonstrated enhanced thermal stability and quantified the inorganic content at approximately 23.7% by mass. The fabricated aptasensor exhibited excellent analytical performance under optimized conditions, with a wide linear concentration range from 0.5 nM to 750 nM ciprofloxacin and a low detection limit of 0.18 nM. The sensor showed remarkable selectivity toward ciprofloxacin against potentially interfering antibiotics and common ions, with relative current responses below 5% for all tested interferents. Good reproducibility with relative standard deviation of 4.3% and repeatability of 3.8% were achieved, indicating the reliability of the fabrication protocol and the robustness of the covalent aptamer immobilization strategy. Storage stability studies revealed that the sensor retained approximately 86% of its initial response after four weeks at 4 °C, demonstrating satisfactory long-term stability for practical applications. Furthermore, the practical applicability of the developed aptasensor was successfully validated through recovery studies in spiked tap water and river water samples, with recoveries ranging from 95.8% to 98.3% and relative standard deviations below 4%. These results confirm that the proposed sensing platform can accurately quantify ciprofloxacin concentrations at trace levels even in complex environmental matrices. The synergistic combination of the highly conductive MWCNT-MoS_2/Ag nanohybrid and the specific recognition properties of the aptamer provides an effective strategy for electrochemical detection of antibiotic residues. This work offers a promising approach for monitoring pharmaceutical contaminants in aquatic environments and contributes to the growing field of nanomaterial-based electrochemical biosensors for environmental analysis.

CONFLICT OF INTEREST

The authors declare that there is no conflict of interests regarding the publication of this manuscript.

REFERENCES

1. Alam AU, Howlader MMR, Hu N-X, Deen MJ. Electrochemical sensing of lead in drinking water using β-cyclodextrin-

modified MWCNTs. Sensors and Actuators B: Chemical. 2019;296:126632.
2. Yang Y, Zhang H, Huang C, Jia N. MWCNTs-PEI composites-based electrochemical sensor for sensitive detection of bisphenol A. Sensors and Actuators B: Chemical. 2016;235:408-413.
3. Wong A, Foguel MV, Khan S, Oliveira FMd, Tarley CRT, Sotomayor MDPT. Development of an Electrochemical Sensor Modified with MWCNT-COOH and MIP For Detection of Diuron. Electrochimica Acta. 2015;182:122-130.
4. Oliveira TMBF, Morais S. New Generation of Electrochemical Sensors Based on Multi-Walled Carbon Nanotubes. Applied Sciences. 2018;8(10):1925.
5. Kan X, Zhang T, Zhong M, Lu X. CD/AuNPs/MWCNTs based electrochemical sensor for quercetin dual-signal detection. Biosensors and Bioelectronics. 2016;77:638-643.
6. Shams A, Yari A. A new sensor consisting of Ag-MWCNT nanocomposite as the sensing element for electrochemical determination of Epirubicin. Sensors and Actuators B: Chemical. 2019;286:131-138.
7. Yari A, Derki S. New MWCNT-Fe_3O_4@PDA-Ag nanocomposite as a novel sensing element of an electrochemical sensor for determination of guanine and adenine contents of DNA. Sensors and Actuators B: Chemical. 2016;227:456-466.
8. Verma D, Chauhan D, Das Mukherjee M, Ranjan KR, Yadav AK, Solanki PR. Development of MWCNT decorated with green synthesized AgNps-based electrochemical sensor for highly sensitive detection of BPA. Journal of Applied Electrochemistry. 2021;51(3):447-462.
9. Kini V, C S S, Mondal D, Sundarabal N, Nag P, Sadani K. Recent advances in electrochemical sensing and remediation technologies for ciprofloxacin. Environmental Science and Pollution Research. 2025;32(5):2210-2237.
10. Adane WD, Chandravanshi BS, Tessema M. A simple, ultrasensitive and cost-effective electrochemical sensor for the determination of ciprofloxacin in various types of samples. Sensing and Bio-Sensing Research. 2023;39:100547.
11. Zokhtareh R, Rahimnejad M, Najafpour-Darzi G, Karimi-Maleh H. A new approach to electrochemical sensing of a wildly used antibiotic; ciprofloxacin. Measurement. 2023;215:112872.
12. Bagheri H, Khoshsafar H, Amidi S, Hosseinzadeh Ardakani Y. Fabrication of an electrochemical sensor based on magnetic multi-walled carbon nanotubes for the determination of ciprofloxacin. Analytical Methods. 2016;8(16):3383-3390.
13. Xiong Y, Zhang D, Ye C, Wang Y, Deng X, Deng D, et al. Ultra-sensitive detection of ciprofloxacin hydrochloride in milk by molecularly imprinted electrochemical sensor based on S-CoFe-MOFs/AuNPs. Journal of Food Composition and Analysis. 2023;122:105439.
14. Shepa J, Király N, Demeterová J, Shepa I, Hviščová P, Volavka D, et al. Determination of ciprofloxacin using metal-organic frameworks-modified electrochemical sensors for environmental and clinical applications. Microchemical Journal. 2025;218:115638.
15. Reddy KR, Brahman PK, Suresh L. Fabrication of high performance disposable screen printed electrochemical sensor for ciprofloxacin sensing in biological samples. Measurement. 2018;127:175-186.
16. Niyitanga T, Evans PE, Ekanayake T, Dowben PA, Jeong HK. Carbon nanotubes-molybdenum disulfide composite for enhanced hydrogen evolution reaction. Journal of Electroanalytical Chemistry. 2019;845:39-47.
17. Arrechea S, Guerrero-Gutiérrez EMA, Velásquez L, Cardona J, Posadas R, Callejas K, et al. Effect of additions of multiwall carbon nanotubes (MWCNT, MWCNT-COOH and MWCNT-Thiazol) in mechanical compression properties of a cement-based material. Materialia. 2020;11:100739.
18. Liu H, Jin F, Liu D, Liu W, Zhao J, Chen P, et al. Preparation and electrochemical performance of MWCNT/MoS_2 composite modified Co–P hydrogen storage material. Solid State Sciences. 2022;131:106952.
19. Miao Y, Xue F, Zhao J, Li M, Ren K, Wu T, et al. Research and Application of Photoacoustic Transducer Based on MWCNT-MoS_2-PDMS Composite Thin Film Layer. Journal of Physics: Conference Series. 2025;2966(1):012012.
20. Bavandpour R, Rajabi M, Asghari A. Electrochemical determination of epirubicin in the presence of topotecan as essential anti-cancer compounds using paste electrode amplified with Pt/SWCNT nanocomposite and a deep eutectic solvent. Chemosphere. 2022;289:133060.
21. Sohouli E, Ghalkhani M, Zargar T, Ahmadi F. Preparation of a Highly Sensitive Electrochemical Aptasensor for Measuring Epirubicin Based on a Gold Electrode Boosted with Carbon Nano-Onions and MB. Biosensors. 2022;12(12):1139.
22. Wang Y, Xie J, Tao L, Tian H, Wang S, Ding H. Simultaneous electrochemical determination of epirubicin and methotrexate in human blood using a disposable electrode modified with nano-Au/MWNTs-ZnO composites. Sensors and Actuators B: Chemical. 2014;204:360-367.
23. Hajian R, Mehrayin Z, Mohagheghian M, Zafari M, Hosseini P, Shams N. Fabrication of an electrochemical sensor based on carbon nanotubes modified with gold nanoparticles for determination of valrubicin as a chemotherapy drug: Valrubicin-DNA interaction. Materials Science and Engineering: C. 2015;49:769-775.
24. Nejad FG, Beitollahi H, Sheikhshoaie I. Electrochemical sensing of methotrexate in the presence of folic acid using PAMAM dendrimer-functionalized multiwalled carbon nanotube-modified electrode. Analytical Methods. 2023;15(26):3196-3205.
25. Heydari-Bafrooei E, Askari S. Electrocatalytic activity of MWCNT supported Pd nanoparticles and MoS_2 nanoflowers for hydrogen evolution from acidic media. International Journal of Hydrogen Energy. 2017;42(5):2961-2969.
26. Ibrahim M, Ibrahim H, Almandil NB, Sayed MA, Kawde AN, Aldaqdouq Y. A Novel Platform Based on Au–CeO_2@MWCNT Functionalized Glassy Carbon Microspheres for Voltammetric Sensing of Valrubicin as Bladder Anticancer Drug and its Interaction with DNA. Electroanalysis. 2020;32(10):2146-2155.
27. Dighole RP, Munde AV, Mulik BB, Dhawale SC, Sathe BR. Multiwalled carbon nanotubes decorated with molybdenum sulphide (MoS_2@MWCNTs) for highly selective electrochemical picric acid (PA) determination. Applied Surface Science. 2024;659:159856.
28. Singh S, Sharma S, Bajwa BS, Kaur I. Hydrothermally synthesized carboxylic acid functionalized multiwalled carbon nanotubes grafted MoS_2 based hybrid composites: Efficient uranium(VI) scavenging sorbents in columns, fabric and matrix membrane systems. Journal of Environmental Chemical Engineering. 2022;10(6):108883.
29. Ramírez-Mondragón E, Contreras OE, Tamayo-Pérez UJ, Oropeza-Guzmán MT. Synthesis and characterization of Ni_2P and MoS_2 on MWCNT as an innovative catalytic material for hydrogen generation. Applied Surface Science. 2020;503:144163.
30. Khan F, Julien CM, Islam SS. Fabrication of multiwalled carbon nanotubes/MoS_2 nanocomposite: Application as temperature sensor. FlatChem. 2023;40:100521.